

Dynamics of Chemical and Charge-Transfer Reactions of Molecular Dications. IV. Proton Transfer and Reactions of Dication Isomers in the $\text{CHCl}^{2+} + \text{D}_2$ System

Jana Roithová,[†] Ján Žabka,[†] Jan Hrušák,[†] Roland Thissen,[‡] and Zdenek Herman^{*,†}

V. Čermák Laboratory, J. Heyrovský Institute of Physical Chemistry, Academy of Sciences of the Czech Republic, Dolejškova 3, CZ-182 23 Prague 8, Czech Republic, and Laboratoire de Chimie Physique, Bât. 350, UMR 8000, Centre Universitaire Paris-Sud, 91 405 Orsay Cedex, France

Received: March 3, 2003; In Final Form: June 19, 2003

Chemical reactions and charge-transfer processes in the $\text{CHCl}^{2+} + \text{D}_2$ system were investigated in crossed-beam scattering experiments. Experimental data were complemented by theoretical calculations of the energetics of the species involved and by calculations of stationary points on the dication potential energy surfaces. The main reaction products were the cations CHCl^+ , CHDCl^+ , and CCl^+ . Integral cross sections for the formation of these species were determined over the collision-energy range of 0.4–2.5 eV (center of mass). Two isomers of the reactant dication were identified, with the H atom being bonded either to a C atom (HCCl^{2+}) or to a Cl atom (CClH^{2+}). The isomer CClH^{2+} , which has a higher ionization energy than HCCl^{2+} , was determined to be responsible for most of the charge-transfer product (the formation of the ground and excited states of CClH^+). The chemical reaction product CHDCl^+ was formed in two processes of different translational-energy release via a long-lived or short-lived intermediate, and it could originate from both reactant dication isomers. The most abundant reaction product, CCl^+ , was formed mostly by a highly exoergic impulsive process of proton transfer from the ground state of the dication HCCl^{2+} to D_2 . This direct reaction of proton transfer seems to be a rather general chemical process in collisions of hydrogen-containing dications with neutrals of some proton affinity.

Introduction

In comparison with the vast amount of data on the kinetics and dynamics of chemical reactions of singly charged ions with molecules, the manifold of information on chemical reactions of dications is very limited. Over the period of 1972–1995, the research concerned only reactions of atomic metal ions,^{1,2} Mg^{2+} ions,³ and Ti^{2+} ions⁴ in flow tube experiments, and of Nb^{2+} ions⁵ and Ta^{2+} and Zr^{2+} ions⁶ in Fourier transform–ion cyclotron resonance (FT–ICR) studies. The occurrence of bond-forming reactions of molecular dications was reported in 1994,⁷ and since then, this exciting class of chemical reactions has been attracting more and more attention, from both experimentalists and theoreticians. Because of the high energy content of most dications (25–40 eV above the respective neutrals), their collision processes result often in the formation of electronically excited species, in subsequent decomposition of internally excited products, and in the formation of pairs of singly charged ions with large relative translational energy. Thus, the energy partitioning in products may differ from both cation–neutral and neutral–neutral reactions. The formation of “naked” fast protons^{8–11} in chemical reactions of molecular dications with hydrogen is yet another unusual feature of these processes.

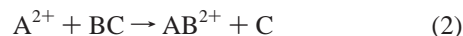
Chemical reactions of dications occur often in competition with charge-transfer processes that lead to the formation

of two singly charged products:

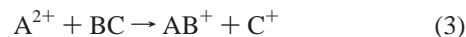


A large amount of data has been obtained on the cross section and energy partitioning in these electron-exchange processes.^{8,12,13}

Chemical reactions of dications can be basically of two types: bond-forming reactions between dications and neutrals, in which a doubly charged ion product and a neutral particle is formed, of the type^{2,14}



or reactions in which two singly charged ions are formed, as a result of bond-rearrangement collisions between a dication and a neutral:



The latter type is particularly interesting, because of an expected high translational-energy release that is due to Coulombic repulsion between the products.

In our earlier communications, we reported crossed-beam scattering studies of the $\text{CF}_2^{2+} + \text{D}_2$ system.^{9,10} Nondissociative processes of charge transfer (reaction 1) and chemical rearrangement, leading to the formation of CF_2D^+ , were shown to be the predominant dication–molecule processes in this system, characterized by high translational-energy release that is due to the Coulomb repulsion between the singly charged

* Author to whom correspondence should be addressed. E-mail: zdenek.herman@jh-inst.cas.cz.

[†] Academy of Sciences of the Czech Republic.

[‡] Centre Universitaire Paris-Sud.

products. A potential energy surface model for reactions of dications with molecules was developed, and this model is based on transitions at the crossings of potential energy surfaces of the dication–neutral system with Coulombic repulsion surfaces of the two singly charged products in the reactant (charge transfer) or product (chemical bond rearrangement) valley. The model accounts for mutual competition of the aforementioned processes (reactions 1–3) in a variety of systems. The predictions of the model were further tested in an experimental and theoretical study of the $\text{CO}_2^{2+} + \text{D}_2$ system.¹¹

In our systematic investigation of the dynamics of chemical reactions and charge-transfer processes of molecular dications, we examined, preliminarily, the reactivity of the CHX^{2+} dications (where X = Cl, Br, CN, OH) in collisions with hydrogen. The $\text{CHCl}^{2+} + \text{D}_2$ system was selected for a more detailed beam scattering study, because both chemical and charge-transfer reactions could be observed in it.

Considerable interest has been devoted in the past years to the structure and stability of substituted methylene CHX^{2+} dications (where X = F, Cl, Br, OH, SH, NH_2).¹⁵ Theoretical and experimental studies of the CH_3X^{2+} and $\text{CH}_2\text{XH}^{2+}$ gas-phase dications^{16,17} provided interesting data on their stability, energetics, and electronic structure. Information on the energetics of several intermediates and products, which are also relevant to this study, can be obtained from a theoretical study¹⁸ of the fragmentation pathways of the chloromethane $\text{CH}_3\text{Cl}^{2+}$ dication.

In this communication, we report results of our crossed-beam scattering studies on elementary reactions of the CHCl^{2+} dication in collisions with deuterium. Earlier information on the ground state of the dication CHCl^{2+} was complemented by our studies of translational-energy spectra from collisions of CHCl^{2+} with Ar, Kr, and Xe atoms¹⁹ and by theoretical calculation of ground and excited states of the dication and the respective cation.²⁰ Analysis of the charge-transfer processes led to the conclusion that two isomers of the CHCl^{2+} dication, with different energetics, were present in the reactant beam, namely HCCl^{2+} and CClH^{2+} .²¹ Some of the theoretical results on the potential energy surface will be presented here; the full extent of the calculations will be published separately.²²

In our experiments on the $\text{CHCl}^{2+} + \text{D}_2$ system at collision energies of 2.16 and 0.82 eV (center of mass, CM), we could identify the cations CHCl^+ , CHDCl^+ , and CCl^+ as reaction products. From the scattering data, contour scattering diagrams were obtained and, from them, angular distributions and relative translational energy distributions of these product ions were extracted. Using these data and combining them with the results of theoretical calculations of the stationary points on the potential energy surfaces, we could describe both nondissociative and dissociative processes of charge transfer and chemical reactions of ground and excited states of the dication reactant and connect them with reaction pathways on the respective potential energy surfaces.

A very important result is the observation of the proton-transfer process from a hydrogen-containing dication to a neutral target (in this case, from CHCl^{2+} to the D_2 reactant, leading to the formation of CCl^+ and HD_2^+). The reaction of proton transfer from hydrogen-containing dications to a neutral target of a certain proton affinity seems to be a rather general process in dication–molecule collisions.

Methods

2.1. Experiments and Data Treatment. The experiments were performed on the EVA II crossed-beam apparatus. The performance and application of the machine to this type of

scattering experiment was described earlier.^{8–11} Briefly, CHCl^{2+} dications were produced via the impact of 130 eV electrons on CH_3Cl in a low-pressure ion source. The ions were extracted, mass-analyzed, and decelerated by a multielement lens to the required laboratory energy. The CHCl^{2+} beam was crossed at right angles with a beam of D_2 molecules emerging from a multichannel jet. The dication beam had angular and energy spreads of 1.2° and 0.5 eV (full width at half-maximum, fwhm), respectively. The collimated neutral beam had an angular spread of 6° (fwhm) and thermal energy distribution at 300 K. Reactant and product ions passed through a detection slit (2.5 cm from the scattering center) into a stopping potential energy analyzer. They were then accelerated and focused into the detection mass spectrometer, mass-analyzed, and detected with the use of a channeltron electron multiplier. Laboratory angular distributions were obtained by rotating the two beams about the scattering center. Modulation of the neutral beam and phase-sensitive detection of the ion products were used to remove background-scattering effects.

Laboratory angular distributions and energy profiles recorded at 6–10 laboratory scattering angles were used to construct scattering diagrams of the investigated products; the contours in the scattering diagrams refer to the Cartesian probability distribution,^{23,24} normalized to the maximum in the particular scattering diagram. CM angular distributions (relative differential cross sections) and relative translational-energy distributions of the products were then obtained in the usual way.^{23,24}

Integral cross sections (in arbitrary units) were obtained in the method described earlier.^{10,11} The ratio of the product ion and the reactant ion intensity, $I_{p,m}/I_{r,m}$, was measured at the ion angular maximum at a series of collision energies and at a constant intensity of the neutral reactant beam. If necessary, the product ion intensities were corrected for a difference in laboratory angular distributions. Under these conditions, the integral cross sections are proportional to the absolute integral cross sections and can be mutually compared.

2.2. Calculations. Calculations of stationary points on the potential energy hypersurface ($\text{CHCl}^{2+} + \text{H}_2$) were performed using the GAUSSIAN 98 program.²⁵ Geometries were fully optimized at the CCSD(T)/cc-pVTZ level.^{26,27} Harmonic frequencies were calculated at each point. Finally, energies of all stationary points were refined using the G2 method.²⁸ Only singlet states relevant to the subject of this paper will be discussed here. The full account of the calculations will be published separately.²² Energetic values for excited states of the dications and cations were calculated using the AQCC approach, as described separately.²⁰ For internal consistency, the energetic and exoergicity values given in this paper are the calculated values. This includes also the ionization energy of H_2 : the calculated G2 value is $\text{IE}(\text{H}_2) = 15.48$ eV (to be compared with tabulated $\text{IE}(\text{H}_2) = 15.43$ eV).

3. Results and Discussion

3.1. Integral Cross Sections. The product ions observed in the studies of the $\text{CHCl}^{2+} + \text{D}_2$ system were the singly charged ions CHCl^+ , CHDCl^+ , and CCl^+ . No measurable amount of the product CD_2Cl^+ could be observed. It can be estimated from the mass spectra that the amount of CD_2Cl^+ was, at all collision energies, <20% of the amount of CHDCl^+ . Figure 1 shows the dependence of the integral cross sections (in arbitrary units) for the formation of these product ions on the collision energy (CM). The formation of CHCl^+ exhibits the smallest cross section. All measured integral cross sections (formation of CHCl^+ , CHDCl^+ , and CCl^+) show an increase at collision

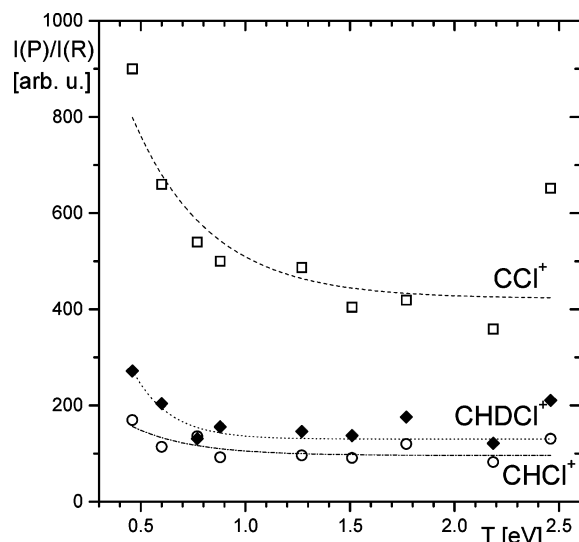


Figure 1. Dependence of the integral cross sections for the formation of (○) CHCl^+ , (◆) CHDCI^+ , and (□) CCl^+ in collisions of CHCl_2^+ with D_2 on the collision energy T .

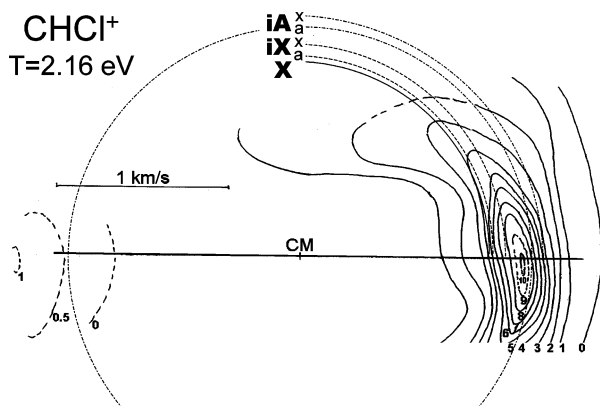


Figure 2. Contour scattering diagram of the charge-transfer product CHCl^+ at the collision energy of 2.16 eV. Solid horizontal line denotes the direction of the relative velocity, whereas CM marks the position of the tip of the center-of-mass velocity vector. Dashed circles show the loci where the product ion should appear if formed in collisions of the dication HCCl_2^+ in the ground state (X), CClH^+ in the ground state (iX), and CClH^+ in the first excited state (iA). See also Figures 4 and 5 and the text.

energies below ~ 1 eV. The data in Figure 1 are in a very good agreement with measurements of the collision-energy dependence of the integral cross sections of formation of these ions by the guided-beam method.²⁹

3.2. Scattering Results. **3.2.1. Formation of CHCl^+ .** The product CHCl^+ is evidently formed in nondissociative charge transfer between the reactants in the reaction



A scattering diagram of CHCl^+ at $T = 2.16$ eV is shown in Figure 2. In this and other scattering diagrams of this paper, the horizontal solid line indicates the direction of the relative velocity vector, and CM denotes the position of the tip of the CM velocity vector. In the CM coordinates, the reactant ion CHCl_2^+ approaches from the left and the neutral reactant approaches from the right.

The product CHCl^+ is scattered predominantly forward of the tip of the CM velocity vector, with only a very small fraction (estimated to be $< 10\%$) scattered backward (the position of the weak backward maximum is indicated only by dashed contours,

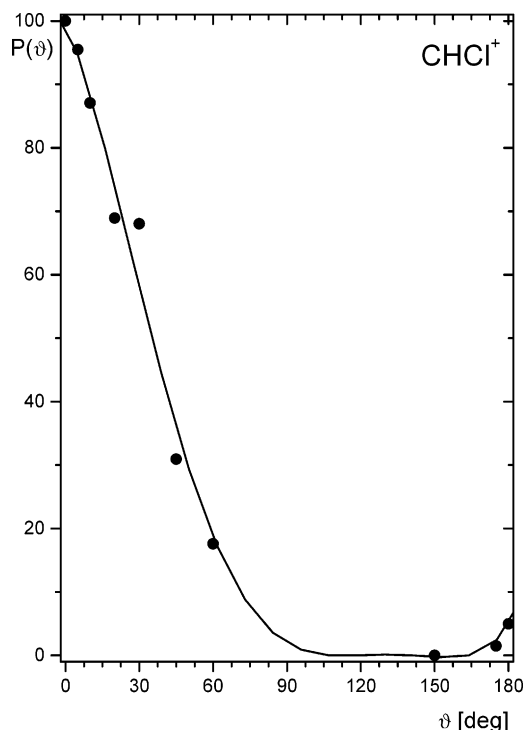


Figure 3. CM angular distribution (relative differential cross section), $P(\vartheta)-\vartheta$, of CHCl^+ at the collision energy of 2.16 eV.

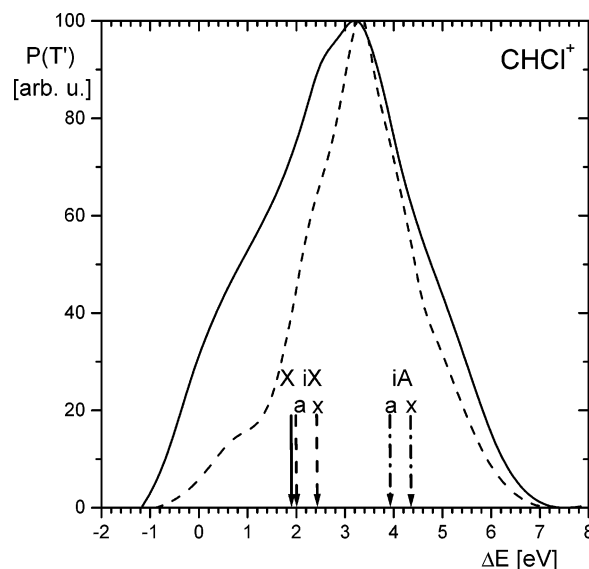


Figure 4. Relative translational-energy distribution, $P(T')$, of charge-transfer products $\text{CHCl}^+ + \text{D}_2^+$ at the collision energy of 2.16 eV plotted against reaction exoergicity $\Delta E = T' - T$ (—) integration over the entire scattering diagram in Figure 2 and (---) $P(T')$ profile in the angular maximum). Arrows indicate adiabatic exoergicities of charge-transfer transitions from the HCCl_2^+ ground state (X) to the HCCl^+ ground state; and from the CClH^+ ground state (iX) and the first excited state (iA) to the CClH^+ ground state (x) and the first excited state (a).

because the data showed some scatter). This behavior is reflected in the CM angular distribution of CHCl^+ in Figure 3. Figure 4 shows the product translational energy distribution, $P(T')$ plotted against the reaction exoergicity, $\Delta E = T' - T$. The data were obtained via the integration of the entire scattering diagram (solid line), and as a profile of the product translational energy distribution at the angular maximum (laboratory scattering angle of -0.2° , dashed line). The unfavorable product mass ratio (a slow heavy ion product recoiling on a light product) makes the energy spectrum rather compressed and not well resolved. The

energy profile at -0.2° is somewhat better resolved, as the integration over the entire diagram includes all the inaccuracies of the experiment.

The low recombination energy of the ground-state CHCl^{2+} (17.39 eV²²) makes the charge-transfer process with D_2 exoergic by only 1.90 eV, below the reaction window; thus, its cross section should be rather low.³⁰ Indeed, the probability of the respective product translational energy is at the lower end of the translational-energy distribution in Figure 4 (see arrow denoted by X in figure). Therefore, the main reactive states of the dication should be, more likely, the electronically excited states. The excited states of the dication HCCI^+ (with the H atom bonded to the C atom) were calculated²⁰ to lie ~ 4 eV above the ground state or higher (an ΔE value of ~ 6 eV or higher in Figure 4). However, Figure 4 clearly shows that the main contribution to the cross section comes from the region of ΔE between 2 and 5 eV.

The problem was resolved by studies of charge transfer between the CHCl^{2+} dication and the noble gases argon, krypton, and xenon.¹⁹ The recoil of the CHCl^+ product on a heavy rare gas ion leads to a much-better-resolved translational-energy spectrum. Briefly, the analysis of the data showed that the CHCl^{2+} dication was formed by electron impact ionization of CH_3Cl in two isomeric forms, $\text{H}-\text{CCl}^{2+}$ (with the H atom bonded to the C atom) and $\text{CCl}-\text{H}^{2+}$ (with the H atom bonded to the Cl atom), present in the reactant beam in an approximate $\text{HCCI}^{2+}:\text{CClH}^{2+}$ ratio of 2:1.¹⁹ The ground and excited states of the isomer CClH^{2+} lie considerably higher in energy than those of HCCI^{2+} and also the states of the CClH^+ isomer cation are located above the states of the HCCI^+ cation. The adiabatic recombination energy of the CClH^{2+} ground state (X $^1\text{A}'$) to the ground state of CClH^+ product is 17.91 eV.²² Excited states of the dication, A $^3\text{A}'$ and B $^3\text{A}''$, lie 1.94 and 2.84 eV above it, respectively.²⁰ Detailed analysis of the data with argon¹⁹ showed that the full account of charge-transfer contributions must include vertical transitions from the first excited state of the CClH^{2+} isomer dication to the ground and the first excited state of the CClH^+ cation.

The adiabatic exoergicities of the respective charge-transfer reactions $\text{CClH}^{2+} \rightarrow \text{CClH}^+$ in collisions with D_2 are shown in Figure 4 by arrows marked by iX and iA (i refers to the isomer CClH^+). The pair of peaks denoted iX refers to transitions from the ground state of the dication to the ground (x) and first excited (a) state of CClH^+ , the pair of peaks denoted iA refers to transitions from the first excited state of the dication to the ground (x) and first excited state (a) of CClH^+ product. In the case of charge transfer with hydrogen, the transitions to the excited state (a) of CClH^+ ($^2\text{A}''$)¹⁹ should be restricted for some collision configurations, because of symmetry reasons. The position of the arrows reflects the translational-energy distribution of products of reaction 1 in a much better way. Taking into account vertical transitions (vibrational excitation of the CClH^+ product of 0.1–0.3 eV and possible vibrational excitation of the D_2^+ product of ~ 0.25 eV¹⁰) shift the arrows slightly to the left to even a better fit.

The conclusion is, therefore, that the cross section of the nondissociative charge transfer (reaction 1) is determined prevalingly by reactions of the $\text{CCl}-\text{H}^{2+}$ isomer. Figure 5 schematically summarizes the energetics of charge-transfer reaction 1 for both isomers, $\text{HCCI}^{2+} \rightarrow \text{HCCI}^+$ and $\text{CClH}^{2+} \rightarrow \text{CClH}^+$. Scattering results at the collision energy of 0.82 eV are consistent with this interpretation.

3.2.2. Formation of CHDCl^+ . A scattering diagram of CHDCl^+ product formed in collisions of CHCl^{2+} with D_2 at a

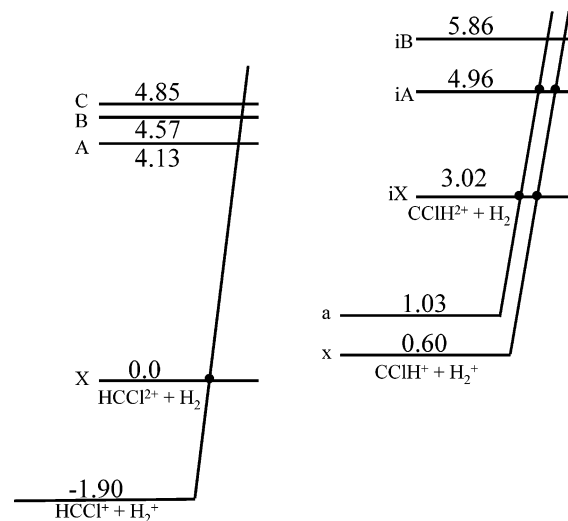


Figure 5. Schematic diagram of energetics of charge-transfer processes of the CHCl^{2+} isomers with D_2 : $\text{HCCI}^{2+} + \text{D}_2$ (left) and $\text{CClH}^{2+} + \text{D}_2$ (right). Dots at crossings refer to processes marked by arrows in Figure 4.

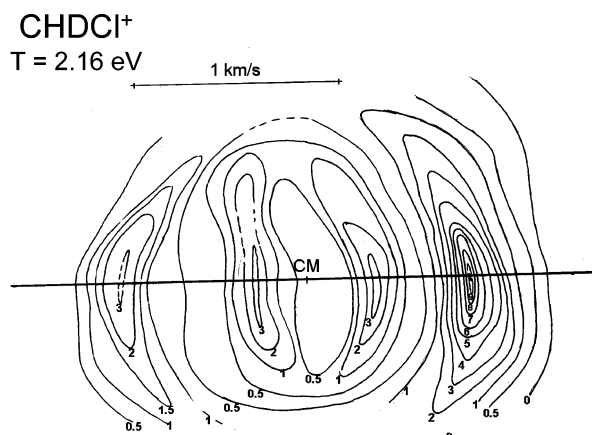
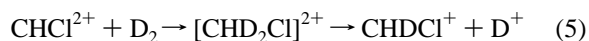


Figure 6. Contour scattering diagram of CHDCl^+ from reaction 5 at the collision energy of 2.16 eV. Designations are analogous to those in Figure 2.

collision energy of 2.16 eV is shown in Figure 6. The scattering is characterized by two pairs of peaks, symmetrically located forward and backward, with respect to the CM. The peaks of the inner pair are $\sim 30\%$ of the maximum intensity and approximately the same height. The outer pair of peaks are unequal in intensity; the forward peak ~ 3 times as high as the backward peak.

The relative differential cross section in Figure 7 shows separately the angular distribution of the product CHCl^+ related to the outer two peaks (solid points) and to the inner peaks (open symbols). Finally, Figure 8 summarizes the translational energy distribution of the products, $P(T')$ vs T' . It exhibits two peaks, at translational energies of ~ 1.1 and 4.7 eV. The lower-energy peak is evidently connected to the inner peaks in the scattering diagram, whereas the higher-energy peak corresponds to the outer peaks in the scattering diagram.

This scattering behavior implies formation of the product by decomposition of intermediates in the reaction



which is characterized by two different translational-energy releases (again, writing H (or D) between C and Cl means the product ion, regardless of the isomeric structures). The process

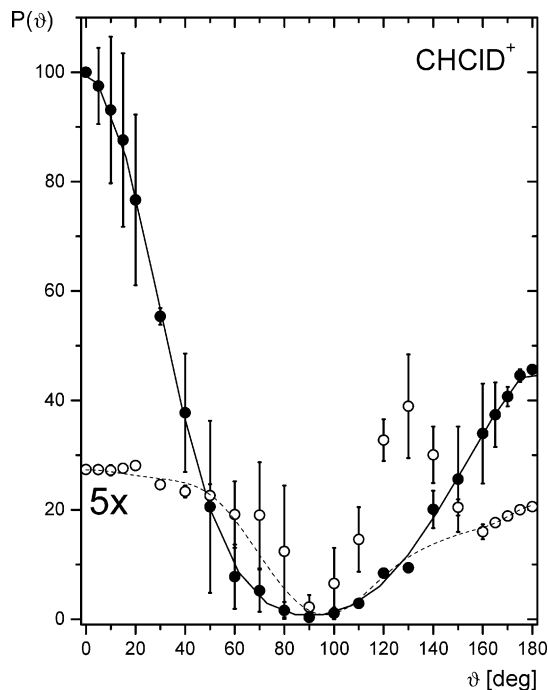


Figure 7. CM angular distributions (relative differential cross sections), $P(\vartheta)-\vartheta$, of CHDCI^+ at $T = 2.16$ eV. Solid line and filled symbols represent integration over the entire scattering diagram; open symbols and dashed line represent integration over the region of the two inner maxima.

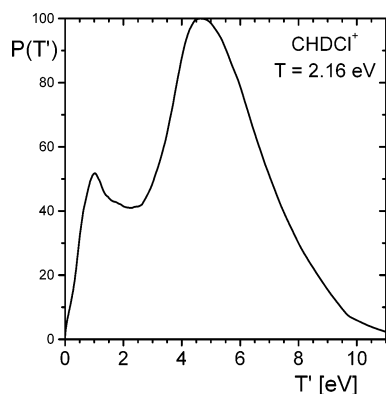


Figure 8. Relative translational-energy distribution, $P(T')-T'$, of products of chemical reaction 5, $\text{CDHCl}^+ + \text{D}^+$, at $T = 2.16$ eV.

with a higher translational-energy release ($T'_{\text{peak}} \approx 4.7$ eV) suggests a decomposition of a shorter-lived intermediate, with an average lifetime of approximately one average rotation (incompletely developed forward-backward symmetry of the scattering pattern, with backward scattering being $\sim 30\%$ of the forward scattering). Strong peaking of the angular distribution in Figure 7 at the CM angle of 0° and 180° implies decomposition of an intermediate via a transition state, which is approximately linear (a prolate transition state^{23,24}). The process with a lower translational-energy release ($T'_{\text{peak}} \approx 1.1$ eV) is less probable and implies the formation of a long-lived intermediate (fully developed forward-backward symmetry) that is associated with a deeper well (in comparison with the former intermediate) on the potential energy surface.

As mentioned earlier, only one product, CHDCI^+ , could be observed, with no measurable intensity of CD_2Cl^+ . In view of the limited resolution, this means that the $\text{CD}_2\text{Cl}^+:\text{CHDCI}^+$ ratio was smaller than ~ 0.2 . This observation implies that, in most reactive collisions, D and H are not equivalent in the intermediate.

A theoretical analysis of the possible reaction paths that lead to the products $\text{CHCl}^+ + \text{D}^+$ is given in Figures 9 and 10. The product evidently can be formed from both isomers of the dication, HCCl^{2+} and CClH^{2+} , via loosely bound complexes, in which the H atom is bonded in a completely different way than the incoming two D atoms. For the HCCl^{2+} reactant ion, there are two possible pathways (Figure 9), both of which involve a rather shallow minimum of -0.93 and -0.23 eV (with respect to the reactants) with expected approximate translational-energy releases of ~ 4.06 and ~ 2.70 eV, respectively (barrier heights from product sites). The latter seems to be less probable, because of a rather high activation barrier, similar to the collision energy (the transition state is located at 1.91 eV, and the barrier height is 2.14 eV). Relevant Rice-Ramsperger-Kassel-Marcus (RRKM) calculations indicate that the average lifetime of the respective intermediates would be on the order of 10^{-12} s, thus corresponding to the short-lived intermediate, as postulated previously. The CClH^{2+} isomer reactant ion can also react via a loosely bound complex with D_2 to form $\text{DCClH}^+ + \text{D}^+$ (Figure 9), with a transitional-energy release up to 3.33 eV (barrier height from the product site). Again, the barrier in the forward direction of 0.92 eV (with a minimum at 1.62 eV and TS at 2.54 eV) would imply a short-lived intermediate.

The pathways that involve the formation of a more-stable ylide intermediate, $\text{H}_2\text{CClH}^{2+}$ (a dication of the ylide form $-\text{H}_2\text{CClH}-$ of methyl chloride), are shown in Figure 10. Again, both reactant dication isomers can react. The HCCl^{2+} dication would give either HDCCl^+ or the mixture of HCClD^+ and DCClD^+ via the ylide intermediate $\text{HDC}-\text{Cl}-\text{D}^{2+}$ (at approximately -3 eV). The relative translational-energy release between the products is 2.8–3.6 eV. However, because of the difference in the barrier heights of the processes, the pathway that involves the higher barrier (1.98 eV) and leads to the mixture of HCClD^+ and DCClD^+ seems to be less likely. The CClH^{2+} isomer would give either DCClH^+ or D_2CCl^+ via pathways that involve formation of the ylide intermediate $\text{D}_2\text{C}-\text{Cl}-\text{H}^{2+}$. The total energy content in this intermediate seems to be very high (at the collision energy of 2.16 eV, this total energy content is ~ 7.8 eV). The calculated translational-energy release for these processes, which involve long-lifetime intermediates (Figure 10), is rather high to account for the low-translational-energy release process observed experimentally (Figures 6 and 8). Therefore, it seems that this process is connected with the formation of an electronic excited state of the product, calculated to be ~ 3.2 eV above the ground-state DHCCl^+ (noted by the dashed line in Figure 10)

In summary, the formation of chemical products in reaction 5 seems to be a rather complicated process that presumably involves both reactant cation isomers, HCCl^{2+} and CClH^{2+} , and several reaction pathways that involve both loosely bound intermediates (average lifetimes of the order of $\sim 10^{-12}$ s) and relatively stable ylide intermediates (lifetimes considerably longer than 10^{-12} s). Assessment of the relative importance of these pathways currently is rather difficult.

Results obtained for the formation of DCClH^+ at the collision energy of 0.82 eV consist of an energy profile of the molecular ion product. They imply a decomposition of an intermediate with two different energy releases, of ~ 0.25 – 0.45 eV and ~ 4.1 eV. Thus, they are in general agreement with the more detailed results at $T = 2.16$ eV, as discussed previously.

3.2.3. Formation of CCl^+ . Figure 11 shows a scattering diagram of the product CCl^+ at the collision energy of 2.16 eV. The diagram shows three peaks. Two of them are located

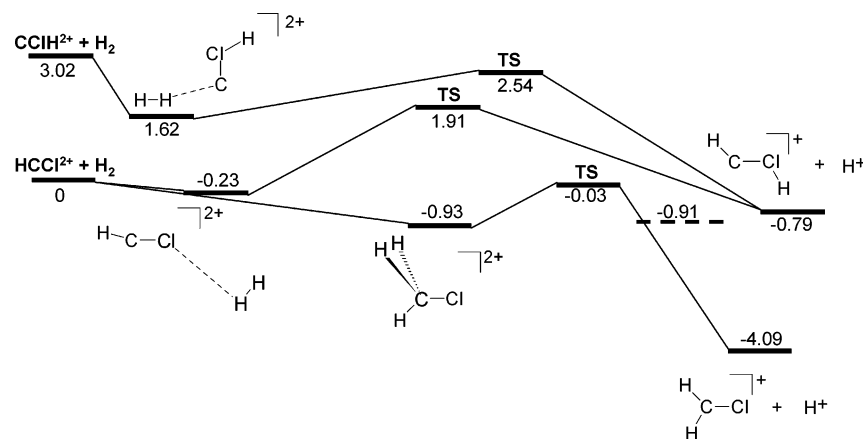


Figure 9. Calculated reaction pathways for chemical reaction 5 involving loosely bound intermediates and shallow minima for both reactant dication isomers, HCCI^{2+} and CCIH^{2+} .

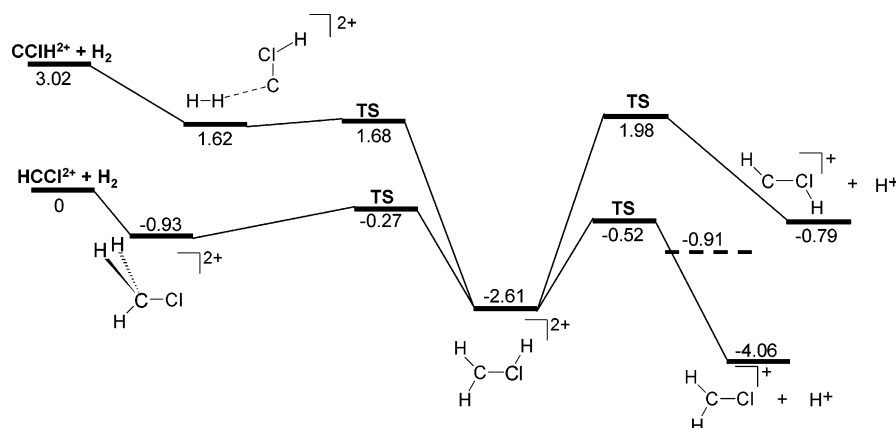


Figure 10. Calculated reaction pathways for chemical reaction 5, involving more-stable ylide intermediates for both reactant dication isomers, HCCI^{2+} and CCIH^{2+} .

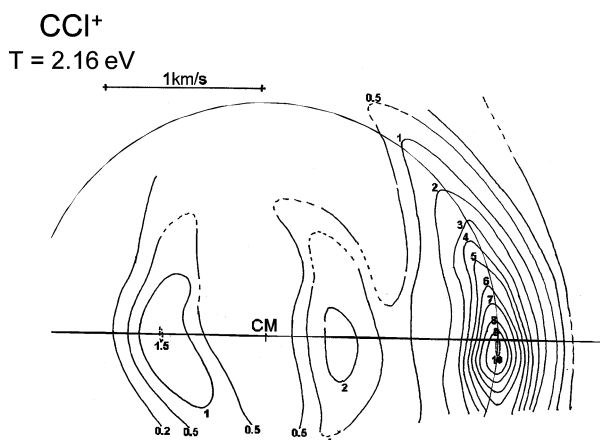


Figure 11. Contour scattering diagram of the product CCl^+ at $T = 2.16$ eV. Designations are analogous to those in Figure 2; the solid circle indicates the product CM velocity through the maximum of the distribution.

symmetrically forward and backward, with respect to the CM at a velocity of ~ 0.5 km/s. The distribution is somewhat asymmetric, with the forward peak (20%) being larger than the backward peak (15%). The preponderant contribution comes from a forward scattered fraction of the product, located at the CM velocity of CCl^+ of ~ 1.5 km/s. Figure 12 brings the relative differential cross section, $P(\vartheta)$ vs ϑ , of the product CCl^+ , obtained by integration of the entire scattering diagram (solid line and solid points) and of the area of the two inner peaks (dashed line and open squares). The $P(\vartheta)$ shape is determined

by the strong forward peak of the more exoergic process; the contribution from the area of the inner peaks is small and contributes to both to the forward and backward scattering. Figure 13 summarizes the evaluation of the distribution of the relative translational energy of the products, $P(T')$, from the scattering diagram in Figure 11. For the sake of discussion of the various possibilities of the formation of CCl^+ , $P(T')$ was plotted as a function of T' for the initial reaction product pair $\text{CHDCl}^+ + \text{D}^+$, the former dissociating further to $\text{CCl}^+ + \text{HD}$ without appreciable energy release (upper scale), and for the reaction product pair $\text{CCl}^+ + \text{HD}_2^+$ (a direct process of proton transfer from CHCl^{2+} to D_2 , lower scale). The low-energy peak of $P(T')$ occurs in the relative translational-energy scale of the initial product pair $\text{CHDCl}^+ + \text{D}^+$ (upper scale and inset) at the low energy of the main peak of the translational-energy distribution of the product pair $\text{CHDCl}^+ + \text{D}^+$ (see Figure 8 and inset in Figure 13). Therefore, CCl^+ in this portion of the translational-energy spectrum may be regarded as a product of a further decomposition of the chemical product CHDCl^+ (reaction 5), namely a further decomposition of the CHDCl^+ from the channel of the higher exoergic (~ 4.7 eV) to $\text{CCl}^+ + \text{HD}$:



An inset in Figure 13 compares the position of the lower-energy peak of CCl^+ (in the T' scale of CHDCl^+ formation) with the translational-energy distribution of CHDCl^+ (from Figure 8). The position of the CCl^+ peak would correspond

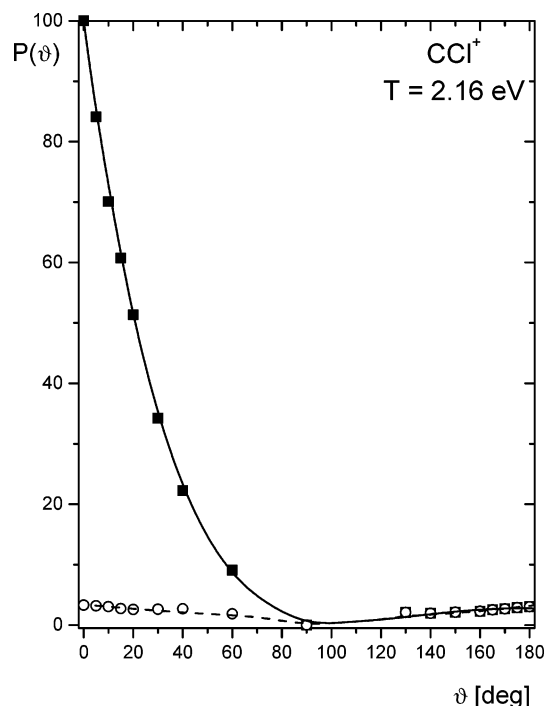


Figure 12. CM angular distributions (relative differential cross sections), $P(\vartheta) - \vartheta$, of CCl^+ at $T = 2.16$ eV; full squares and solid line represent integration over the entire scattering diagram in Figure 11, whereas open circles and dashed line represent integration over the region of the two inner maxima.

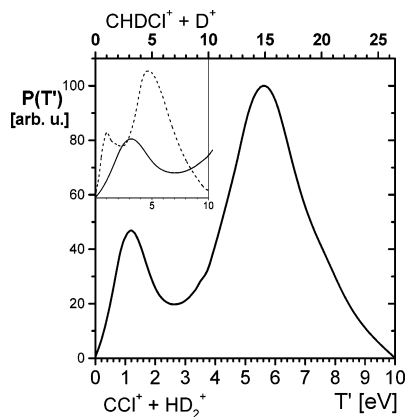
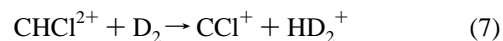


Figure 13. Relative translational-energy distribution, $P(T') - T'$, of products leading to CCl^+ at $T = 2.16$ eV. The relative translational energy T' was calculated for the primary reaction product pair $\text{CHDCI}^+ + \text{D}^+$ (from which CCl^+ is assumed to originate in a subsequent dissociation, upper scale) and for the reaction product pair $\text{CCl}^+ + \text{HD}_2^+$ (lower scale). Inset shows a comparison of (—) the present $P(T')$ curve with (---) the $P(T')$ curve from Figure 8 for the product ion pair $\text{CHDCI}^+ + \text{D}^+$ (see text).

rather well to further decomposition of the chemical product CHDCI^+ , formed in the higher-energy-release reaction and possessing large internal energy (lower end of the translational-energy distribution). A certain forward–backward asymmetry of the scattering (20% vs 15%, respectively) of this fraction of CCl^+ is in reasonable agreement with the asymmetry of the outer peaks of the CHDCI^+ products (100% vs 30%, respectively; see Figure 6). However, the exoergicity of the higher-energy release process of CCl^+ formation in the translational-energy coordinates for the $\text{CHDCI}^+ - \text{D}^+$ product pair (~ 15 eV) is unreasonably large in this computation. Therefore, one must look for another reaction mechanism to form this preponderant fraction of CCl^+ .

This reaction mechanism for the formation of the product CCl^+ with high translational-energy release (the peak at $T' = 5.6$ eV, lower-energy scale) is a proton-transfer reaction



with an exoergicity of 5.30 eV (calculated value; see Section 2.2). The distribution of CCl^+ , which is associated with this process, in the scattering diagram (Figure 11) is strongly forward with an unmeasurable small backward component, estimated to be smaller than $\sim 5\%$ of the forward peak, which suggests an impulsive direct process. A firm identification of this process would be the observation of HD_2^+ as the other reaction product. This is, however, not easy in the scattering experiments: most of HD_2^+ is scattered in the opposite direction than CCl^+ , i.e., backward, with respect to the original dication movement, and, thus, in the experimentally inaccessible region backward in the laboratory frame of reference. Nonetheless, one could barely identify a peak of HD_2^+ at m/z 5, which is slightly higher than the background noise (as a result of the portion of very weak scattering that corresponded to backward scattering of CCl^+). However, a clear identification of both products CCl^+ and HD_2^+ was made in complementary guided-beam experiments in which integral cross sections of the reactions in the $\text{CHCl}^+ + \text{D}_2$ system were determined.²⁹

The proton-transfer reaction is a commonly observed reaction in collisions of multiprotonated biomolecules (polypeptides) with neutral targets^{35,36} or negative ions.³⁷ Although it has not been described so far for reactions of small molecular dications, it may be a rather general process in hydrogen-containing molecular dication–neutral collisions. So far, we also have been able to identify it in the reaction of CHCl^{2+} with argon ($\text{CCl}^+ + \text{ArH}^+$ formation^{19,29}) and, more recently, in reactions of the dication $\text{C}_4\text{H}_3^{2+}$ with a series of atomic and molecular targets.³⁸

4. Conclusions

Experimental studies (crossed-beam scattering) and theoretical calculations (energetics of dication and cation species involved, stationary points on the $(\text{CHCl}-\text{H}_2)^{2+}$ hypersurface) of the $\text{CHCl}^{2+} + \text{D}_2$ system lead to the following conclusions:

(1) The main products of chemical reactions and charge-transfer processes in the system are the singly charged ions CHCl^+ , CHDCI^+ , and CCl^+ .

(2) The integral cross sections (in arbitrary units) of these products were determined over the collision-energy range of 0.4–2.5 eV (center of mass, CM). The integral cross section for the charge-transfer product CHCl^+ , for the chemical products CHDCI^+ and CCl^+ , shows an increase at collision energies < 1 eV. The collision-energy dependence of the integral cross sections from these experiments is in good agreement with the results of the guided-beam experiments.

(3) The translational-energy release in the charge-transfer process with D_2 could be explained by the existence of two isomers of the reactant dication CHCl^{2+} in the beam— $\text{H}-\text{CCl}^{2+}$ and $\text{CCl}-\text{H}^{2+}$ —of different energetics, as confirmed by theoretical calculations. The isomer CClH^{2+} is mostly responsible for the formation of the charge-transfer product CClH^+ in the ground and excited states. Important support for this conclusion comes from simultaneous experimental and theoretical studies of charge-transfer processes between CHCl^{2+} and argon, krypton, and xenon.¹⁹

(4) CHDCI^+ was formed in two processes of a different translational-energy release (~ 1.0 and ~ 4.7 eV at $T = 2.16$ eV). The former process is associated with a long-lived

intermediate formation, whereas the latter process is associated with a formation of a short-lived intermediate. Both isomers of the reactant dication can contribute to the product formation. The possible pathways have been analyzed on the basis of theoretical calculations of the stationary points on the hyper-surface $(\text{CHCl}-\text{D}_2)^{2+}$. However, the complexity of this seemingly simple system makes specific assignment of the reaction paths very difficult.

(5) The most abundant product CCl^+ results from a proton-transfer reaction, mostly from the ground state of the dication HCCl^{2+} , in a direct, impulsive process of a rather high exoergicity. This may be a general process in dication–molecule chemical reactions.

(6) Both ground and excited states of the two isomers, HCCl^{2+} and CClH^{2+} , participate in the reactions. The excited-state (iA) of CClH^{2+} contributes significantly to the nondissociative charge transfer, and the proton transfer seems to result primarily from the reaction of the ground state of HCCl^{2+} .

Acknowledgment. Partial support of this research by Grant No. 203/00/0632 from the Grant Agency of the Czech Republic, Grant No. IAB4040302 from the Grant Agency of the Academy of Sciences, the French–Czech Cooperation Program KONTAKT-Barrande No. 2002-013-1, and the European Network MCI (Generation, Structure and Reaction Dynamics of Multiply-Charged Ions) is gratefully acknowledged. One of the authors (R.T.) expresses his thanks for a stipend of the MCI Network Program.

References and Notes

- Weisshaar, J. C. *Acc. Chem. Res.* **1993**, *26*, 231 and references therein.
- Roth, L. M.; Freiser, B. S. *Mass Spectrom. Rev.* **1991**, *10*, 303.
- Spears, K. G.; Fehsenfeld, G. C.; McFarland, M.; Ferguson, E. E. *J. Chem. Phys.* **1972**, *56*, 2562.
- Tonkyn, R.; Weisshaar, J. C. *J. Am. Chem. Soc.* **1986**, *108*, 7128.
- Gord, J. R.; Freiser, B. S.; Buckner, S. W. *J. Chem. Phys.* **1989**, *91*, 7530.
- Ranasinghe, Y. A.; MacMahon, T. M.; Freiser, B. S. *J. Phys. Chem.* **1991**, *95*, 7721.
- Price, S. D.; Manning, M.; Leone, S. R. *J. Am. Chem. Soc.* **1994**, *116*, 8673.
- Herman, Z. *Int. Rev. Phys. Chem.* **1996**, *15*, 299.
- Dolejšek, Z.; Fárník, M.; Herman, Z. *Chem. Phys. Lett.* **1995**, *235*, 99.
- Herman, Z.; Žabka, J.; Dolejšek, Z.; Fárník, M. *Int. J. Mass Spectrom.* **1999**, *192*, 191.
- Mrázek, L.; Žabka, J.; Dolejšek, Z.; Hrušák, J.; Herman, Z. *J. Phys. Chem. A* **2000**, *104*, 7294.
- Mathur, D. *Phys. Rep.* **1993**, *225*, 193.
- Herman, Z. *Phys. Essays* **2000**, *13*, 480.
- Lu, W.; Tosi, P.; Bassi, D. *J. Chem. Phys.* **2000**, *112*, 4648.
- Wong, M. W.; Yates, B. F.; Nobes, R. H.; Radom, L. *J. Am. Chem. Soc.* **1987**, *109*, 1381 and earlier references therein.
- Maquin, F.; Stahl, D.; Sawaryn, A.; Schleyer, P. v. R.; Koch, W.; Frenkin, G.; Schwarz, H. *J. Chem. Soc., Chem. Commun.* **1984**, 504.
- Ruhl, E.; Price, S. D.; Leach, S.; Eland, J. H. D. *Int. J. Mass Spectrom. Ion Process.* **1990**, *97*, 175.
- Duflot, D.; Robbe, J.-M.; Flament, J.-P. *Int. J. Mass Spectrom. Ion Process.* **1997**, *171*, 215.
- Roithová, J.; Žabka, J.; Thissen, R.; Herman, Z. *Phys. Chem. Chem. Phys.* **2003**, *5*, 2988.
- Roithová, J.; Hrušák, J.; Herman, Z. *Int. J. Mass Spectrom.* **2003**, *228*, 497.
- Throughout this paper, the formula CHCl^{n+} (with H between C and Cl) is used whenever the isomers are not distinguished, and HCCl^{n+} or CClH^{n+} is used whenever a reference to a particular isomer of the dication ($n = 2$) or cation ($n = 1$) is made.
- Roithová, J.; Hrušák, J.; Herman, Z. *J. Phys. Chem. A* **2003**, *107*, 7355.
- Friedrich, B.; Herman, Z. *Collect. Czech Chem. Commun.* **1984**, *49*, 590.
- Herman, Z. *Int. J. Mass Spectrom.* **2001**, *212*, 413.
- Frisch, M. J.; Trucks, G. W.; Schlegel, H. B.; Scuseria, G. E.; Robb, M. A.; Cheeseman, J. R.; Zakrzewski, V. G.; Montgomery, J. A., Jr.; Stratmann, R. E.; Burant, J. C.; Dapprich, S.; Millam, J. M.; Daniels, A. D.; Kudin, K. N.; Strain, M. C.; Farkas, O.; Tomasi, J.; Barone, V.; Cossi, M.; Cammi, R.; Mennucci, B.; Pomelli, C.; Adamo, C.; Clifford, S.; Ochterski, J.; Petersson, G. A.; Ayala, P. Y.; Cui, Q.; Morokuma, K.; Malick, D. K.; Rabuck, A. D.; Raghavachari, K.; Foresman, J. B.; Cioslowski, J.; Ortiz, J. V.; Stefanov, B. B.; Liu, G.; Liashenko, A.; Piskorz, P.; Komaromi, I.; Gomperts, R.; Martin, R. L.; Fox, D. J.; Keith, T.; Al-Laham, M. A.; Peng, C. Y.; Nanayakkara, A.; Gonzalez, C.; Challacombe, M.; Gill, P. M. W.; Johnson, B. G.; Chen, W.; Wong, M. W.; Andres, J. L.; Head-Gordon, M.; Replogle, E. S.; Pople, J. A. *Gaussian 98*, revision A.6; Gaussian, Inc.: Pittsburgh, PA, 1998.
- Pople, J. A.; Head-Gordon, M.; Raghavachari, K. *J. Chem. Phys.* **1987**, *87*, 5968.
- Kendall, R. A.; Dunning, T. A., Jr.; Harrison, R. J. *J. Chem. Phys.* **1992**, *96*, 6796.
- Curtiss, L. A.; Raghavachari, K.; Trucks, G. W.; Pople, J. A. *J. Chem. Phys.* **1991**, *94*, 7221.
- Roithová, J.; Thissen, R.; Žabka, J.; Franceschi, P.; Dutuit, O.; Herman, Z. *Int. J. Mass Spectrom.* **2003**, *228*, 487.
- The “reaction window” concept was developed^{8,31–33} to account for the fact that reaction rates (cross section) for charge transfer between dications and atoms have a tendency to be large for processes with rather large exoergicities (several electron volts), rather than for processes with exoergicities that are approximately zero, as in cation–atom (molecule) charge transfer. It is based on the Landau–Zener model³⁴ of electron-transfer adiabatic transitions. This model works rather well for most dication–neutral electron transfer processes that are characterized by well-localized crossings of the reactant term (relatively flat ion-induced dipole interaction, combined with repulsive short-distance interaction) and the product term (steep Coulomb repulsion). If the crossing occurs at large internuclear separations, the two terms cross diabatically and the transition probability is small; if they cross at small internuclear separations, the terms are adiabatically split and the probability of crossing to the product potential energy system is small again. It is only if the probability of a single-passage crossing is ~ 0.5 (intermediate internuclear separations) that the system has a good chance of ending on the potential energy system of the two singly charged products. This happens for crossing at ~ 2.5 – 5.5 Å, depending on the collision energy, or for reaction exoergicities of 2.6–5.8 eV.^{8,33}
- Spears, K. G.; Fehsenfeld, F. C.; McFarland, F.; Ferguson, E. E. *J. Chem. Phys.* **1972**, *56*, 2562.
- Lindinger, W.; Smith, D. In *Reactions of Small Transient Species* (and references therein); Fontijn, A., Clyne, M. A. A., Eds.; Academic Press: New York, 1983.
- Lindinger, W.; Hansel, A.; Herman, Z. *Adv. At. Mol. Opt. Phys.* **2000**, *43*, 243.
- Nikitin, E. E.; Umanskii, S. Y. *Theory of Slow Atomic Collisions*; Springer–Verlag: Berlin, 1984.
- Williams, E. R. *J. Mass Spectrom.* **1995**, *31*, 831.
- Schnier, P. D.; Gross, D. S.; Williams, E. R. *J. Am. Chem. Soc.* **1995**, *117*, 6747.
- McLuckey, S. A.; Stephenson, J. L. *Mass Spectrom. Rev.* **1998**, *17*, 369.
- Jašík, J.; Ipolyi, I.; Roithová, J.; Žabka, J.; Thissen, R.; Herman, Z., to be published.